HHS Public Access

Author manuscript

Gastroenterology. Author manuscript; available in PMC 2020 January 01.

Published in final edited form as:

Gastroenterology. 2019 January ; 156(1): 160–174.e7. doi:10.1053/j.gastro.2018.09.050.

Tropism for Spasmolytic Polypeptide-Expressing Metaplasia Allows *Helicobacter pylori* to Expand its Intra-gastric Niche.

José B. Sáenz[1], **Nancy Vargas**[1], and **Jason C. Mills**[1,2,3]

[1]Division of Gastroenterology, Department of Internal Medicine, Washington University in St. Louis School of Medicine

[2]Department of Pathology and Immunology, Washington University in St. Louis School of Medicine

[3]Department of Developmental Biology, Washington University in St. Louis School of Medicine

Abstract

BACKGROUND AND AIMS: In patients with chronic *Helicobacter pylori* (*H pylori)* infection, parietal and chief cell atrophy in the gastric corpus, a process known as spasmolytic polypeptide-expressing metaplasia (SPEM), increases the risk for progression to cancer. The relationship between *H pylori* and these metaplastic changes is unclear. We investigated whether *H pylori* localizes to regions of SPEM.

METHODS: We developed an *in situ* adherence assay in which we incubated *H pylori* with free-floating tissue sections from the gastric corpora of mice; we assessed *H pylori* distribution along the gastric unit by immunofluorescence. We analyzed the interactions of *H pylori* with tissue collected from mice with acute SPEM, induced by high-dose tamoxifen. We also evaluated how adhesin-deficient *H pylori* strains, chemical competition assays, and epithelial glycosylation affected *H pylori* adhesion to SPEM glands. Finally, we colonized mice with the mouse-adapted PMSS1 strain and analyzed *H pylori* colonization *in vivo* during tamoxifen-induced SPEM or after reduction of stomach acid with omeprazole.

RESULTS: Compared to uninjured glands, *H pylori* penetrated deep within SPEM glands, *in situ*, via interaction of its adhesin, SabA, with sLex, which expanded in SPEM. *H pylori* markedly increased gastric corpus colonization when SPEM was induced, but this proximal spread reversed in mice allowed to recover from SPEM. Reducing corpus acidity also promoted proximal spread.

Correspondence: Jason C. Mills, Division of Gastroenterology, Department of Internal Medicine, Washington University in St. Louis School of Medicine, 660 S. Euclid Avenue, Campus Box 8124, St. Louis, MO 63110, 314-362-4213, 314-362-7487 (fax), jmills@wustl.edu.

Author Contributions: JBS designed and performed experiments, analyzed and interpreted data, performed statistical analyses, provided some of the funding for the study, and drafted and critically revised the manuscript. NV designed and performed experiments, analyzed and interpreted data, and critically revised the manuscript. JCM provided most of the funding for the study and critically revised the manuscript.

Disclosures: None of the authors have any financial disclosures.

Conflict(s) of Interest: None to declare.

However, *H pylori* penetrated deep within corpus glands *in vivo* only when sLex expanded during SPEM.

CONCLUSIONS: *H pylori* differentially binds SPEM glands *in situ* and in mice, in large part by interacting with sLex. Our findings indicate that *H pylori* expands its niche into the gastric corpus by promoting and exploiting epithelial metaplastic changes that can lead to tumorigenesis.

Graphical Abstract

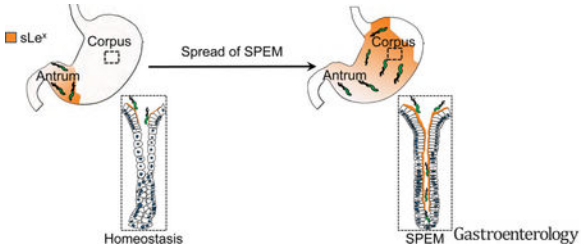

Keywords

paligenosis; intestinal metaplasia; patients; stomach cancer

INTRODUCTION

Infection with the Gram-negative bacterium *Helicobacter pylori* (*H pylori*) remains the most significant risk factor for the development of gastric adenocarcinoma, one of the leading causes of cancer-related deaths worldwide. An increased risk for progression to the often fatal endpoint of gastric neoplasia begins in patients who exhibit substantial loss of acid-secreting parietal cells, a process known as oxyntic atrophy, in the setting of chronic inflammation. This chronic atrophic gastritis is associated with a reorganization of the gastric unit, characterized by increased proliferation of gastric progenitor cells in the isthmus of the gastric unit (between the upper pit/foveolar cells and the deeper cells of the gland) and the reprogramming of post-mitotic chief cells at the base of the gastric gland into a proliferating population of metaplastic cells. The pattern of gastric unit reorganization during chronic atrophy is often referred to as spasmolytic polypeptide-expressing metaplasia (SPEM)4. It is thought to normally represent an evolutionarily conserved, transient alteration in the gastric unit of the proximal stomach (*i.e.,* corpus) to facilitate repair and restoration of normal architecture in the face of deep glandular injury. In some cases, however, restoration is blocked, and persistent SPEM can progress to gastric dysplasia.

SPEM can expand topographically (anatomically) in the stomach via the gradual extension of an atrophic front, or a zone of progressive inflammation and metaplasia. In humans, it is thought that SPEM first occurs at the transition between the antrum and corpus and moves proximally into the corpus, spreading most rapidly along the lesser curvature, . The extension of the atrophic front into the gastric corpus has clinical significance. In particular, patients with *H pylori*-induced gastritis and atrophy/SPEM involving the gastric corpus are at a heightened risk of progressing to gastric adenocarcinoma.

The ability of *H pylori* to expand its intra-gastric niche into the gastric corpus has often been attributed to a decrease in gastric acidity following chronic inflammation; while *H pylori* can survive in acidic conditions, it does not effectively colonize the intensely acidic gastric corpus. At the glandular level, *H pylori* attaches to gastric epithelium primarily through the binding of two bacterial adhesins, BabA and SabA, to the glycosylated receptors Lewis B (Le^b) and sialyl-Lewis X (sLe^x), respectively, on host epithelium. How the dynamic equilibrium between host and microbial factors determines the topographic (*i.e.*, corpus versus antrum) distribution of *H pylori*, a critical determinant of neoplastic risk, has not been systematically explored. Notably, in patients demonstrating extensive corpus atrophy/metaplasia, it remains unclear whether *H pylori* expands into the corpus due to changes in epithelial expression patterns characteristic of SPEM, with parietal cells and chief cells being replaced by metaplastic cells, or whether *H pylori* simply extends into the relatively less acidic environment resulting from the gradual loss of parietal cells.

In this study, we attempt to address for the first time the mechanism(s) behind *H pylori*'s expansion into the atrophic corpus and its direct interactions with SPEM glands. We first take advantage of a validated gastric injury model that rapidly, synchronously, and reversibly induces SPEM throughout the corpus[9] . Using a novel *in situ* binding assay where we can manipulate host and microbial factors, we find that *H pylori* differentially binds deep within SPEM glands compared to normal corpus glands and that this binding is in part dependent on the interaction of SabA with sLe^x. We expand our *in situ* assay to a mouse model of *H pylori* colonization to demonstrate that the SabA-sLe^x interaction also determines *H pylori*'s ability to extend into the corpus and bind deep within SPEM glands *in vivo*. Finally, we demonstrate that omeprazole-mediated inhibition of gastric acid allows *H pylori* to spread to the corpus but without penetrating deeper within corpus glands. Our results elucidate a mechanism by which *H pylori* exploits the metaplastic changes within the corpus that accompany chronic inflammation to expand its niche at a topographic and glandular level. As the differentiation changes associated with metaplasia pose a risk for the accumulation of mutations[9] , *H pylori*'s tropism for SPEM glands could contribute to the establishment of a pre-neoplastic gastric milieu.

MATERIALS AND METHODS

Ethical Permissions

All human gastric specimens were obtained with approval from the Institutional Review Board of Washington University School of Medicine. All experiments involving animals were performed according to protocols approved by the Washington University School of Medicine Animal Studies Committee. Mice were maintained in a specified pathogen-free barrier facility under a 12-hour light cycle.

In Situ H pylori adherence assay

Male and female littermates were given two daily intra-peritoneal injections with either vehicle or high-dose tamoxifen (HD-Tam; 5 mg/20 g body weight), as previously described. Mice were sacrificed one or fourteen (recovery) days after the last injection. Mouse stomachs were excised, inflated with 4% paraformaldehyde (PFA), and fixed overnight at

4°C with gentle rocking. The next day, the forestomach was removed, and stomachs were cut open along the lesser curvature prior to embedding in 4% low-melting agarose. 100-μm longitudinal sections from the gastric corpus were cut using a vibratome (Leica Biosystems, Vista, CA) and blocked overnight at 4°C in phosphate-buffered saline (PBS) containing 3% bovine serum albumin. Free-floating sections were incubated with overnight *H pylori* cultures (see Supplemental Methods) diluted in blocking buffer to an OD_{600} of 0.05, unless otherwise indicated. Sections were incubated in each well of a 48-well plate (Greiner Bio-One, Monroe, NC) for 1 hour at 37°C and 5% CO_2 with gentle shaking (30 rpm), then transferred to a new well and washed three times with sterile PBS prior to fixing in 4% PFA for 1 hour at room temperature.

Immunofluorescence

Thick (100-μm), fixed sections were blocked for 2 hours in blocking buffer (PBS, 3% bovine serum albumin, 1% Triton X-100, 1% saponin), then incubated overnight at 4°C in the appropriate primary antibody. Sections were washed and incubated in the appropriate secondary antibodies for 2 hours at room temperature. Sections were then incubated in Hoescht stain (1:20,000; Thermo Fisher Scientific) for 30 minutes at room temperature, transferred to a microscope slide, and mounted using ProLong Gold antifade reagent (Thermo Fisher Scientific). Images were obtained using the Olympus FV1200 confocal microscope (Olympus, Waltham, MA), and z-stacks were reconstructed into three-dimensional images using Amaris software (Thermo Fisher Scientific).

Assessing Depth of Penetration

Intra-glandular bacteria were determined by confocal microscopy. The number of glands containing intra-glandular *H pylori* bacteria located at or below the level of *Griffonia simplicifolia* lectin (GSII) staining (below the pit region) was expressed as a percentage of the total colonized glands. Approximately 80–100 *H pylori*-colonized glands were counted for each of three consecutive, independent experiments. For colonized glands containing more than one bacterium, the location of the deepest bacterium was counted.

Determining Topographic Distribution of *H pylori*

Male and female littermates aged 6–8 weeks were infected with PMSS1 (~1×10^8 cfu/mouse) for 6 weeks, after which they were intra-peritoneally injected with vehicle or HD-Tam, as described above. For omeprazole treatment, mice were infected for 6 weeks, then gavaged daily for one week with 200 μL of either saline (Hospira Inc., Lake Forest, IL) or an omeprazole slurry (Sigma; 1.5 mg/20 g body weight resuspended in saline) prior to sacrifice. For all treatments, mouse stomachs were excised and cut open along the lesser curvature. The forestomach was removed, food was gently scraped away, and exposed stomachs were cut into three equal horizontal sections: proximal corpus (closest to forestomach), distal corpus, and antrum (closest to intestine). Each gastric section was placed in sterile Brucella broth, weighed, and homogenized for 30 seconds in N°10 Medicons (Beckto n Dickinson, San Jose, CA). Dilutions were plated on selective media plates (tryptic soy agar with 5% sheep blood) containing amphotericin (2 μg/mL), bacitracin (30 μg/mL), nalidixic acid (10 μg/mL), and vancomycin (20 μg/mL). Plates were incubated under micro-aerophilic conditions in Ziploc bags containing GasPak EZ sachets (Becton Dickinson and Company,

Franklin Lakes, NJ) at 37°C for 5–7 days. Colonies were counted and expressed as colony-forming units per gram of stomach (cfu/g stomach).

Statistical Analysis

All graphs and statistical analyses were done using GraphPad Prism (GraphPad, La Jolla, CA). Means among multiple (> 2) treatments were compared using one-way analysis of variance with the Dunnett's test to determine significance. When calculating bacterial densities in infected mice, the adjusted means and standard deviations were calculated for replicates that fell below the level of detection using Cohen's method. Means for bacterial densities and glandular distributions in saline- versus omeprazole-treated mice were compared using a one-tailed Student's *t* test. $P < 0.05$ was considered statistically significant. Where indicated, *, $p< 0.05$; ** $p < 0.01$; *** $p < 0.001$; **** $p < 0.0001$; n.s., not significant ($p > 0.05$).

RESULTS

H pylori *differentially binds to SPEM glands* in situ

We first sought to use a controlled *in situ* system to study how *H pylori* differentially interacts with atrophic/SPEM-type metaplastic corpus. To generate metaplastic tissue for our assay, we employed an acute, drug-induced gastric injury model that causes nearly all parietal cells to die and corpus units to undergo SPEM within three days of injury. Equally important, this synchronous injury system is reversible, with near complete recovery to normal corpus within two weeks. As previously reported, intra-peritoneal administration of high-dose tamoxifen (HD-Tam; 5 mg/20 g body weight) to wild-type C57BL/6 mice results in a rapid induction of SPEM throughout the mouse stomach, characterized by the co-expression of the murine chief cell marker, gastric intrinsic factor (GIF), and the mucous neck cell marker, GSII, at the gland base (Figures 1A–B). HD-Tam induced similar gastric injury in male and female mice, as has been previously reported. The acute loss of acid-secreting parietal cells in HD-Tam-treated mice (Supplemental Figure 1A) resulted in mucosal atrophy and pallor, evidenced by a loss in the anatomic distinction between corpus and antrum (Supplemental Figure 1B) as well as by a rise in intra-gastric pH (Supplemental Figure 1C). The histologic, morphologic, and functional changes associated with HD-Tam-induced SPEM were reversible, as glands recovering from HD-Tam injury reverted to the vehicle-treated phenotype at the glandular and gross anatomic levels (Figure 1C and Supplemental Figure 1B).

The rapidity and reversibility of the HD-Tam injury system allowed us to assess the direct interactions between *H pylori* and the reconfigured gastric epithelium by examining *H pylori*'s interaction with gastric tissue harvested both during SPEM and after recovery from injury. Previous attempts at studying *H pylori* adherence to gastric epithelium largely relied on incubating slides containing thin, deparaffinized sections of murine or human gastric tissue with *H pylori*[5] . We developed a novel *in situ* adherence assay using thick gastric sections. Compared to previous studies, the use of thicker, free-floating, 100-μm sections facilitated analysis of depth of penetration and enhanced spatial resolution of *H pylori* binding to gastric epithelium. While *in situ* binding of the mouse-adapted PMSS1 isolate of

H pylori was largely restricted to the pit region of vehicle-treated glands, *H pylori* were able to bind more deeply along the gastric unit axis in SPEM glands, and this phenotype was lost when *H pylori* were incubated with gastric glands from mice that had recovered from SPEM (Figures 1D–I).

To quantify the differences in the depth of *H pylori* binding to normal versus metaplastic glands, we determined the number of glands containing *H pylori* adherent to the gastric unit deep to the pit region (*i.e.,* within the glandular region of the corpus unit) and normalized to the total number of glands containing bound *H pylori*. Immunofluorescent images were analyzed by confocal microscopy to ensure that *H pylori* deep within a gland were indeed within the glandular lumen (Supplemental Movie 1). For glands containing more than one *H pylori* bacterium, the location of the intra-glandular bacterium found deepest within the gastric unit was scored. *H pylori* more frequently bound below the pit/foveolar region of SPEM glands (HD-Tam) compared to vehicle-treated glands (68% vs 37%, respectively; $p < 0.001$; Figure 1J). The depth of binding of *H pylori* to glands that had recovered from SPEM was not significantly different from the pattern seen with vehicle-treated glands (32% vs 37%, respectively; $p > 0.05$; Figure 1J). Taken together, these findings demonstrate that *H pylori* binds deeper within SPEM glands *in situ* and that this binding is reversible following recovery from HD-Tam-induced glandular injury.

Sialyl-Lewis X (sLe^x) expression is expanded in SPEM

We next hypothesized that *H pylori*'s differential binding to SPEM glands was the result of the enhanced expression of a receptor for *H pylori* on host gastric epithelium following HD-Tam injury. *H pylori* has been shown to adhere to gastric epithelium through the binding of two of its adhesins, BabA and SabA, to the blood group antigen Lewis b (Le^b) and sialylated Lewis X (sLe^x), respectively. No difference in the pattern of Le^b expression was seen between vehicle- and HD-Tam-treated glands, suggesting that HD-Tam-induced SPEM did not alter glandular Leb expression (Figure 2A). SPEM induction, however, drastically enhanced the expression of sLe^x, which extended deep into the metaplastic neck and gland base, identified by GIF and GSII co-staining (Figure 2B). This staining pattern was lost following recovery from HD-Tam injury, with the scant sLe^x expression in recovered glands resembling that of vehicle treatment.

H pylori *binding to SPEM glands is α-linkage-specific and is mediated by binding of SabA to* sLe^x

In our *in situ* adherence assay, *H pylori* co-localized with epithelial cells showing increased sLe^x expression within SPEM glands (Figures 2C–D). To demonstrate that the binding of *H pylori* to SPEM glands *in situ* was mediated by the direct interaction of SabA with its cognate receptor, sLe^x, we incubated SPEM glands with *H pylori* in the presence of one of two glycoconjugates that differentially binds terminal sialic acid residues on gastric epithelium. SabA has been previously shown to bind α−2,3-linked terminal sialic acid residues on sLe^x . Consistent with this, increasing concentrations of the glycoconjugate 3'-sialyllactose, which preferentially binds α−2,3-linked terminal sialic acid residues, significantly inhibited the ability of *H pylori* to bind deep within SPEM glands in a dose-dependent manner (Figure 3). However, an enantiomeric glycoconjugate, 6'-sialyllactose,

which preferentially binds α−2,6-linked terminal sialic acid residues, had no effect on the ability of *H pylori* to bind deep within SPEM glands, suggesting that the binding of *H pylori* to SPEM glands *in situ* is α-linkage-specific. Similarly, the ability of *H pylori* to penetrate deep within SPEM glands was abolished if the tissue sections were pre-treated with neuraminidase, which specifically cleaves terminal sialic acid residues; accordingly, neuraminidase pre-treatment also significantly reduced binding of *Maackia amurensis* lectin, which recognizes α−2,3-linked terminal sialic acid residues on sLex, to SPEM glands (Supplemental Figure 2).

Because sLe^x availability on host gastric tissue affected *H pylori* binding to SPEM glands, we wanted to further confirm the role of the *H pylori* adhesin, SabA, in binding metaplastic gastric tissue. We assessed the *in situ* binding of a wild-type clinical *H pylori* strain, NSH57, or isogenic mutants lacking either SabA (*ΔsabA*), BabA (*ΔbabA*), or both SabA and BabA (*ΔsabA/ΔbabA*). These strains have been previously characterized, and no differences were seen among the strains in terms of *in vitro* growth or motility (not shown). Similar to the PMSS1 strain (Figure 1E), the wild-type NSH57 strain adhered deep within SPEM glands (Figure 4A), though the frequency at which NSH57 was found below the pit region (53%; Figure 4E) was slightly lower than that observed with the PMSS1 strain (68%; Figure 1J). Nonetheless, the *ΔsabA* mutant could not bind deep within SPEM glands as effectively as its isogenic wild-type counterpart (35% vs 53%, respectively; $p < 0.05$; Figures 4B and 4E). Notably, the *ΔbabA* mutant bound deep within SPEM glands to a similar extent as the wild-type, isogenic NSH57 strain (Figures 4C and 4E), while the mutant lacking both adhesins (*ΔsabA/ΔbabA*) showed no appreciable binding to SPEM glands *in situ* (*i.e.,* fewer than 5% of glands showed bound *H pylori* anywhere along the gland axis; Figures 4D–E). Taken together, these results suggest that *H pylori* binding to SPEM glands is an active and specific process that depends on both of the *H pylori* adhesins, BabA and SabA, but the ability to penetrate deep within SPEM glands depends in large part on the ability of SabA to bind sLe^x.

SPEM affects the topographic and glandular distribution of H pylori *in vivo*

To demonstrate that the interactions observed *in situ* were important for *H pylori* pathogenesis *in vivo*, we first examined mice that had been chronically infected with PMSS1 and noticed an expansion of sLe^x expression in glands undergoing SPEM (Figures 5B–C), similar to the expression pattern seen in HD-Tam-induced SPEM (Figure 2B). Moreover, this pattern of sLe^x expression was restricted to injured corpus glands undergoing SPEM and was not a non-specific mucosal response to chronic *H pylori* infection, as sLe^x expression was not enhanced in uninjured, non-colonized corpus mucosa within the same infected mouse stomach (Figure 5A). Of note, HD-Tam-induced SPEM did not cause the expansion of foveolar/pit cells observed in SPEM induced by chronic inflammation; hence, *H pylori*-infected gastric units with SPEM showed longer spans of sLe^x-expressing foveolar regions.

Similar to the mouse, we also consistently observed that in regions of human SPEM/atrophy, sLe^x expanded into the bases of SPEM glands (Figures 5F–I and Supplemental Figures 5B–D). In uninjured human glands, sLe^x was confined to the surface and shallow foveolar regions without extending deep within the gastric unit (Figure 5D and Supplemental Figure

5A). sLe^x was also not expressed in regions of intestinal metaplasia (Figures 5E and Supplemental Figure 5C). A summary of the sLe^x staining pattern in human gastric specimens with varying histopathology is presented in Supplemental Table 1.

Given that glandular sLe^x is expanded in SPEM glands and that *H pylori* reversibly binds SPEM glands through its interactions with sLe^x, we reasoned that the presence of SPEM could determine *H pylori*'s gastric colonization patterns during chronic infection. Taking advantage of the fact that HD-Tam induces synchronous SPEM throughout the gastric corpus and that this injury is reversible, we could assess *H pylori* colonization patterns following manipulation of the gastric landscape. We developed a method for assessing *H pylori* colonization of distinct topographic regions of infected mouse stomachs in the presence or absence of SPEM. Male and female littermate mice were infected with PMSS1 for 6 weeks, intra-peritoneally injected with vehicle or HD-Tam for 2 days, then sacrificed either one or fourteen days after the last injection. Excised stomachs were cut open along the lesser curvature, and *H pylori* was isolated and quantified from three distinct regions of the mouse stomach (see Methods). Treatment with HD-Tam allowed *H pylori* to more effectively colonize the proximal and distal regions of the gastric corpus compared to vehicle-treated mice (Figures 6A–B). HD-Tam injury appeared to have no effect on *H pylori* density within the gastric antrum (Figure 6C), consistent with SPEM representing an injury response of the gastric corpus. More importantly, this pattern of colonization was reversible, with *H pylori* redistributing away from the proximal corpus following recovery from HD-Tam injury. These findings suggest that the presence of SPEM dictates *H pylori*'s ability to colonize more proximal regions of the gastric corpus and that *H pylori* redistributes away from the corpus following recovery from SPEM.

While the topographic, or anatomic, distribution of *H pylori* within the infected stomach has clinical significance, the distribution of *H pylori* within colonized glands may be equally relevant for the host epithelial response and the establishment of a pre-neoplastic micro-environment. To assess how SPEM altered the glandular distribution of *H pylori in vivo*, we analyzed paraffin-embedded gastric corpus sections from chronically infected, vehicle- or HD-Tam-treated mice (see Supplemental Methods). The distance of *H pylori* along the gland axis was expressed as a percentage of the total gland length under the different treatment conditions (Figure 6D). For the recovery experiment, mice were sacrificed fourteen days after the last HD-Tam injection. Similar to our *in situ* findings (Figures 1D–J), *H pylori* was able to access deeper portions of metaplastic corpus glands following the induction of SPEM with HD-Tam. However, the *H pylori* foray deep within injured corpus glands was reversed in mice allowed to recover from SPEM (Figure 6E). In further corroboration of our *in situ* findings, sLe^x expression expanded along the gland unit in *H pylori* -colonized SPEM glands following HD-Tam treatment, while in stomachs that had recovered from SPEM and were no longer colonized deep within the gland, sLe^x staining reverted to the vehicle control pattern (Figures 6F–I).

SPEM, and not inhibition of acid secretion, determines H pylori's *glandular distribution* in vivo

Treatment with HD-Tam induces a rapid loss of parietal cells (Supplemental Figure 1A) and an expected rise in intra-gastric pH (Supplemental Figure 1C). It has previously been hypothesized that it is the change in intra-gastric pH that allows for the proximal expansion of *H pylori* from the antrum into the corpus. Thus, we decided to formally test the relative contribution of metaplasia and acid to *H pylori* colonization. To test the effect of gastric pH on *H pylori* colonization patterns, PMSS1-infected littermates were gavaged daily with either saline or omeprazole. Regional bacterial densities were determined, as previously described. Similar to HD-Tam treatment, omeprazole treatment significantly enhanced *H pylori* colonization of the proximal and distal corpus compared to saline controls (Figures 7A–B), with no significant effect on colonization of the antrum (Figure 7C). However, omeprazole alone failed to induce SPEM (Supplemental Figure 3). Accordingly, unlike HD-Tam (Figure 7E), omeprazole treatment did not stimulate an expansion of sLe^x expression deep within the corpus gland axis (Figure 7D). Moreover, consistent with the pit-restricted sLe^x expression pattern following omeprazole treatment, the glandular distribution of *H pylori* in omeprazole-treated mice was not significantly different from saline-treated littermates (Figure 7G). These findings indicate that *H pylori*'s colonization of the gastric corpus may be impeded by acid, but it is specifically the presence of SPEM that dictates *H pylori*'s ability to penetrate deep within corpus units.

DISCUSSION

In this study, we used a combination of *in situ* and *in vivo* models to systematically examine the interaction of *H pylori* with a changing corpus landscape. The atrophic and metaplastic changes that *H pylori* both induces and leverages are what allows it, in some patients, to cause gastric cancer, so the questions that we have addressed in this study are critical for understanding this clinically relevant aspect of *H pylori* pathogenesis. We brought new tools to bear on this problem, with the acute, reversible metaplastic injury caused by HD-Tam allowing us to alter the gastric environment in a synchronous manner in the absence of chronic inflammation.

The *in situ H pylori* adherence assay allowed us to directly manipulate and compare *H pylori*'s interactions with uninjured and metaplastic glands in the absence of active acid secretion. However, we caution that this interaction is not the sole determinant of *H pylori*'s interaction with SPEM glands, as the Δ*sabA* mutant was still able to deeply penetrate approximately one third of SPEM glands. The *in situ* adherence assay is thus an oversimplification of *H pylori*'s binding to gastric epithelium. Fixed tissue lacks active acid secretion, local pH gradients, and infiltrating host immune cells, all relevant factors that dynamically influence *H pylori* pathogenesis *in vivo*.

Nonetheless, the *in vivo* experiments validated the significance of *H pylori*'s interactions with SPEM glands observed *in situ.* While it has been previously reported that chronically inflamed gastric tissue manifests expanded sLe^x , the cellular context of this expansion has not been studied – namely, that it specifically occurs in SPEM glands. Furthermore, it has not been clear how altering the gastric landscape by inducing SPEM and expanded sLe^x

affects *H pylori* pathogenesis directly. The ability of *H pylori* to directly and reversibly bind SPEM glands through SabA's interaction with expanded sLe^x represents a dynamic adaptation of *H pylori* to a chronic inflammatory environment that has significant implications for *H pylori* colonization *in vivo*.

Previous analysis of the host determinants that dictate *H pylori*'s topographic distribution and oncogenic risk has largely been correlative. Indeed, chronic acid suppression through the use of proton pump inhibitors had been shown to promote a multi-focal gastritis in humans, and mice infected with *H pylori*, though the pre-neoplastic implications of gastritis distribution patterns were not pursued. We demonstrate that *H pylori*'s colonization of the metaplastic corpus is fluid, with the bacteria redistributing away from the most proximal regions of the corpus following recovery from HD-Tam injury. One could argue that these changes in *H pylori* distribution within the stomach are simply the result of changes in gastric acidity, as HD-Tam treatment raises intra-gastric pH within the range of omeprazole treatment. Indeed, omeprazole-induced acid suppression, like HD-Tam treatment, promoted a more efficient colonization of the gastric corpus in mice, and a similar phenomenon has been observed in humans on chronic acid suppression.

However, our findings equally indicate that *H pylori*'s distribution within the depths of the gastric corpus unit depends on the injury state of the gland, not simply on loss of gastric acidity. Inhibition of gastric acid secretion *in vivo* did not alter the distribution of *H pylori* within each gland; specifically, it did not promote binding deep within corpus glands. Instead, it was the presence of SPEM, presumably in large part because of the concomitant expansion of sLe^x toward the gland base, that dictated whether *H pylori* could access deeper regions along the gastric corpus unit.

Distinguishing the topographic distribution of *H pylori* from its glandular distribution may be relevant from a pathophysiologic standpoint. The glandular changes that characterize the gastric epithelial injury response that is SPEM involve cellular reprogramming and proliferation along the metaplastic gland axis; lectins have been shown to mark various cells and differentiation patterns in gut epithelial lineages. We demonstrate that the pattern of sLe^x expression in human gastric specimens is specific to SPEM but does not mark another gastric pre-neoplastic lesion, intestinal metaplasia. The role of increased sLe^x expression during SPEM remains unclear, though it may mark a transient return to an oncofetal state as part of a conserved injury response in the gastric corpus. Our evolving understanding of SPEM as a glandular injury response implicates cellular plasticity as a key underlying mechanism governing the response of the damaged corpus unit. Indeed, we have previously shown that there is a conserved cellular program, paligenosis, whereby post-mitotic, differentiated cells can revert to an oncofetal state by first scaling down mature cellular features, then re-expressing more primitive cell surface markers (*e.g.*, SOX9 and, presumably, sLe^x), and finally proliferating in order to efficiently repair the gland.

From a microbial perspective, one could make the teleological argument that *H pylori* has adapted to exploit the host's glandular repair mechanisms by specifically, and perhaps preferentially, binding SPEM glands. Colonization deep within SPEM glands could serve to protect *H pylori* from the harsher, more acidic environment near the gastric lumen. As sLe^x

expression deep within the gland is lost during injury repair, *H pylori* is forced out of this micro-environment and must seek to establish a new niche, perhaps in adjacent injured glands. The changes in the pattern of sLe^x expression that accompany SPEM provide a means by which the spread of *H pylori* parallels that of SPEM. *H pylori* may encourage the spread of SPEM throughout the stomach, either indirectly by inducing chronic inflammation that causes this metaplastic repair response, or directly by injecting toxins like CagA that affect epithelial differentiation. Thus, *H pylori* can advance throughout the stomach by following, and binding, an advancing front of inflammation and SPEM, marked in part by expanded sLe^x.

From a clinical perspective, the ability of *H pylori* to bind deep within and interact with injured corpus epithelium, characterized by enhanced sLe^x expression, could potentially lead to an accumulation of mutations within metaplastic cells undergoing cycles of proliferation and differentiation changes as part of glandular repair, as we and others have proposed[,] . Indeed, enhanced sLe^x expression is a marker of poor prognosis in gastric adenocarcinoma. Overall, *H pylori*'s interaction with sLe^x in SPEM glands during chronic inflammation would not only be a crucial determinant of its natural history within a host but would also have important implications for the establishment of a pre-neoplastic gastric milieu that contributes to the patient's overall oncogenic risk.

Supplementary Material

Refer to Web version on PubMed Central for supplementary material.

ACKNOWLEDGMENTS:

We thank James Fitzpatrick and Dennis Oakley (Washington University Center for Cellular Imaging) for technical assistance with confocal imaging. We would also like to thank Hei-Yong (Grant) Lo for help with the intra-gastric pH measurements.

Grant support: J.C.M. is supported by National Institute of Diabetes and Digestive and Kidney Diseases awards DK094989, DK105129, and DK110406, by the Alvin J. Siteman Cancer Center–Barnes Jewish Hospital Foundation Cancer Frontier Fund, NIH National Cancer Institute P30 CA091842, and by the Barnard Trust. J.B.S. holds a Postdoctoral Enrichment Program Award from the Burroughs Wellcome Fund and is also supported by the American Gastroenterology Association Gastric Cancer Foundation Research Scholar Award.

REFERENCES:

1. Ferlay J, Soerjomataram I, Dikshit R, et al. Cancer incidence and mortality worldwide: sources, methods and major patterns in GLOBOCAN 2012. Int J Cancer 2015;136:E359–86. [PubMed: 25220842]
2. Correa P, Piazuelo MB. The gastric precancerous cascade. J Dig Dis 2012;13:2–9. [PubMed: 22188910]
3. Nam KT, Lee HJ, Sousa JF, et al. Mature chief cells are cryptic progenitors for metaplasia in the stomach. Gastroenterology 2010;139:2028–2037 e9. [PubMed: 20854822]
4. Schmidt PH, Lee JR, Joshi V, et al. Identification of a metaplastic cell lineage associated with human gastric adenocarcinoma. Lab Invest 1999;79:639–46. [PubMed: 10378506]
5. Willet SG, Mills JC. Stomach Organ and Cell Lineage Differentiation: from Embryogenesis to Adult Homeostasis. Cell Mol Gastroenterol Hepatol 2016;2:546–559. [PubMed: 27642625]

6. Goldenring JR, Nam KT, Wang TC, et al. Spasmolytic polypeptide-expressing metaplasia and intestinal metaplasia: time for reevaluation of metaplasias and the origins of gastric cancer. Gastroenterology 2010;138:2207–10, 2210 e1. [PubMed: 20450866]
7. Graham DY. History of Helicobacter pylori, duodenal ulcer, gastric ulcer and gastric cancer. World J Gastroenterol 2014;20:5191–204. [PubMed: 24833849]
8. Saenz JB, Mills JC. Acid and the basis for cellular plasticity and reprogramming in gastric repair and cancer. Nat Rev Gastroenterol Hepatol 2018;15:257–273. [PubMed: 29463907]
9. Amieva M, Peek RM, Jr. Pathobiology of Helicobacter pylori-Induced Gastric Cancer. Gastroenterology 2016;150:64–78. [PubMed: 26385073]
10. Lee A, Dixon MF, Danon SJ, et al. Local acid production and Helicobacter pylori: a unifying hypothesis of gastroduodenal disease. Eur J Gastroenterol Hepatol 1995;7:461–5. [PubMed: 7614109]
11. Boren T, Falk P, Roth KA, et al. Attachment of Helicobacter pylori to human gastric epithelium mediated by blood group antigens. Science 1993;262:1892–5. [PubMed: 8018146]
12. Mahdavi J, Sonden B, Hurtig M, et al. Helicobacter pylori SabA adhesin in persistent infection and chronic inflammation. Science 2002;297:573–8. [PubMed: 12142529]
13. Huh WJ, Khurana SS, Geahlen JH, et al. Tamoxifen induces rapid, reversible atrophy, and metaplasia in mouse stomach. Gastroenterology 2012;142:21–24 e7. [PubMed: 22001866]
14. Leushacke M, Tan SH, Wong A, et al. Lgr5-expressing chief cells drive epithelial regeneration and cancer in the oxyntic stomach. Nat Cell Biol 2017.
15. Mills JC, Sansom OJ. Reserve stem cells: Differentiated cells reprogram to fuel repair, metaplasia, and neoplasia in the adult gastrointestinal tract. Sci Signal 2015;8:re8.
16. Saenz JB, Burclaff J, Mills JC. Modeling Murine Gastric Metaplasia Through Tamoxifen-Induced Acute Parietal Cell Loss. Methods Mol Biol 2016;1422:329–39. [PubMed: 27246044]
17. Pentecost M, Otto G, Theriot JA, et al. Listeria monocytogenes invades the epithelial junctions at sites of cell extrusion. PLoS Pathog 2006;2:e3. [PubMed: 16446782]
18. Cohen AC. Simplified Estimators for the Normal Distribution When Samples Are Singly Censored or Truncated. Technometrics 1959;1:217–237.
19. Falk P, Roth KA, Boren T, et al. An in vitro adherence assay reveals that Helicobacter pylori exhibits cell lineage-specific tropism in the human gastric epithelium. a 1993;90:2035–9.
20. Magalhaes A, Rossez Y, Robbe-Masselot C, et al. Muc5ac gastric mucin glycosylation is shaped by FUT2 activity and functionally impacts Helicobacter pylori binding. Sci Rep 2016;6:25575. [PubMed: 27161092]
21. Juge N Microbial adhesins to gastrointestinal mucus. Trends Microbiol 2012;20:30–9. [PubMed: 22088901]
22. Hirmo S, Kelm S, Schauer R, et al. Adhesion of Helicobacter pylori strains to alpha-2,3-linked sialic acids. Glycoconj J 1996;13:1005–11. [PubMed: 8981092]
23. Talarico S, Whitefield SE, Fero J, et al. Regulation of Helicobacter pylori adherence by gene conversion. Mol Microbiol 2012;84:1050–61. [PubMed: 22519812]
24. Logan RP, Walker MM, Misiewicz JJ, et al. Changes in the intragastric distribution of Helicobacter pylori during treatment with omeprazole. Gut 1995;36:12–6. [PubMed: 7890214]
25. Bugaytsova JA, Bjornham O, Chernov YA, et al. Helicobacter pylori Adapts to Chronic Infection and Gastric Disease via pH-Responsive BabA-Mediated Adherence. Cell Host Microbe 2017;21:376–389. [PubMed: 28279347]
26. Syder AJ, Guruge JL, Li Q, et al. Helicobacter pylori attaches to NeuAc alpha 2,3Gal beta 1,4 glycoconjugates produced in the stomach of transgenic mice lacking parietal cells. Mol Cell 1999;3:263–74. [PubMed: 10198629]
27. Peterson WL. Helicobacter pylori and gastric adenocarcinoma. Aliment Pharmacol Ther 2002;16 Suppl 1:40–6.
28. Kuipers EJ, Lundell L, Klinkenberg-Knol EC, et al. Atrophic gastritis and Helicobacter pylori infection in patients with reflux esophagitis treated with omeprazole or fundoplication. N Engl J Med 1996;334:1018–22. [PubMed: 8598839]

29. Danon SJ, O'Rourke JL, Moss ND, et al. The importance of local acid production in the distribution of Helicobacter felis in the mouse stomach. Gastroenterology 1995;108:1386–95. [PubMed: 7729630]

30. Weis VG, Goldenring JR. Current understanding of SPEM and its standing in the preneoplastic process. Gastric Cancer 2009;12:189–97. [PubMed: 20047123]

31. Falk P, Roth KA, Gordon JI. Lectins are sensitive tools for defining the differentiation programs of mouse gut epithelial cell lineages. Am J Physiol 1994;266:G987–1003. [PubMed: 8023947]

32. Karam SM, Li Q, Gordon JI. Gastric epithelial morphogenesis in normal and transgenic mice. Am J Physiol 1997;272:G1209–20. [PubMed: 9176232]

33. Willet SG, Lewis MA, Miao ZF, et al. Regenerative proliferation of differentiated cells by mTORC1-dependent paligenosis. EMBO J 2018;37.

34. Koeppel M, Garcia-Alcalde F, Glowinski F, et al. Helicobacter pylori Infection Causes Characteristic DNA Damage Patterns in Human Cells. Cell Rep 2015;11:1703–13. [PubMed: 26074077]

35. Futamura N, Nakamura S, Tatematsu M, et al. Clinicopathologic significance of sialyl Le(x) expression in advanced gastric carcinoma. Br J Cancer 2000;83:1681–7. [PubMed: 11104566]

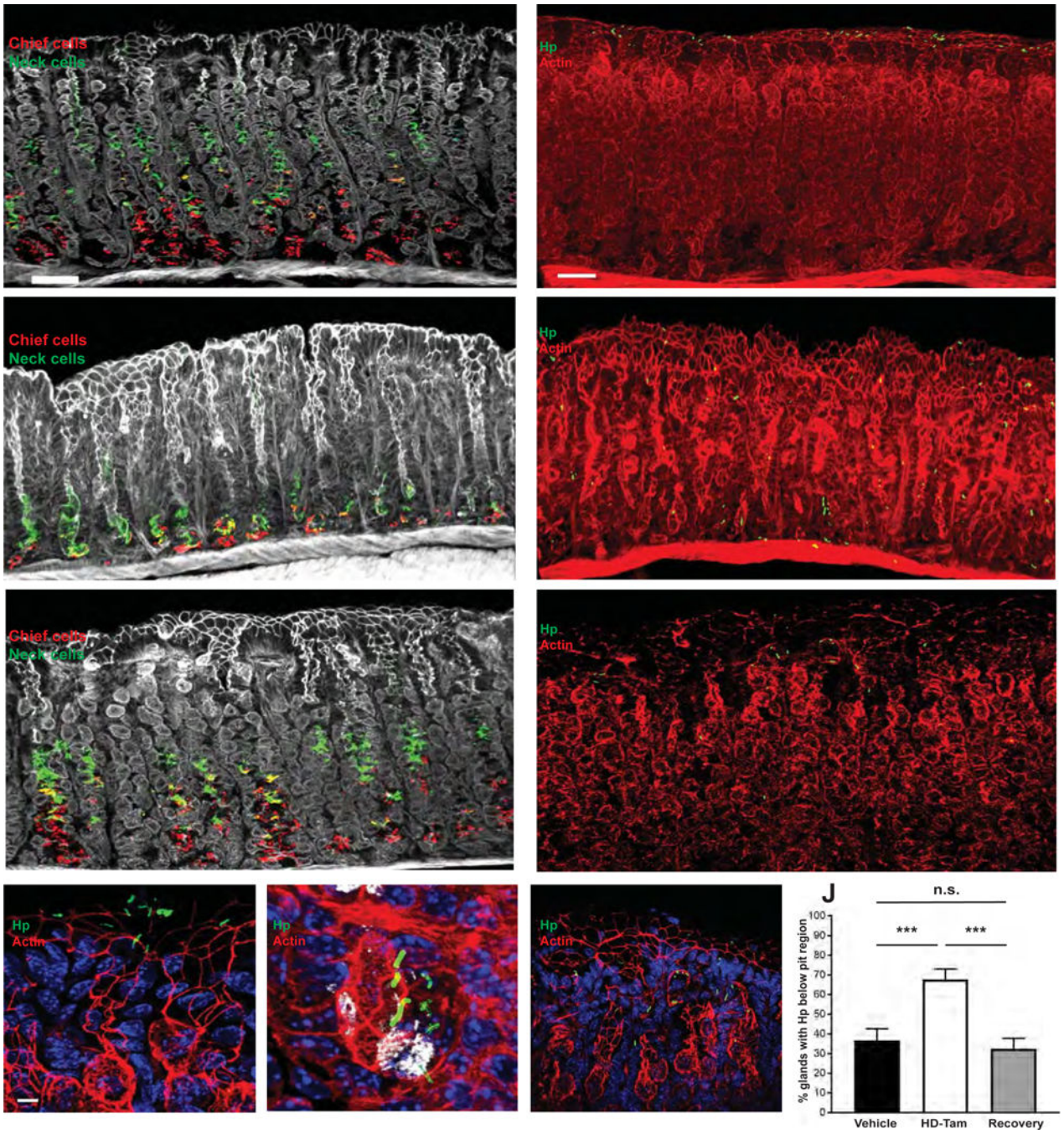

Figure 1. *H pylori* differentially binds SPEM glands *in situ*.

*(*A-C*)* HD-Tam treatment rapidly induces co-expression of chief cell (red) and mucous neck cell (green) markers at the base of corpus glands, changes characteristic of SPEM, but this effect is lost following recovery from SPEM. Thick gastric corpus sections from mice intraperitoneally injected with either vehicle (A) or HD-Tam (B), or allowed to recover (C; see Methods) were imaged by confocal microscopy. White, actin. Scale bar, 50 μm. (D–F) *H pylori* is able to bind deep within SPEM glands (E) but is largely restricted to the pits of vehicle-treated (D) or recovered (F) glands. Scale bars, 50 μm. (G–I) Magnified,

representative images showing *H pylori* within the pits of vehicle-treated (G) and recovered glands (I) but near the base of HD-Tam-treated glands (H). GSII (white) labels the base of SPEM glands. Scale bars, 3 μm. For (D–I), blue labels nuclei, red labels actin. (J) Data show the mean (±SD) percentage of glands containing *H pylori* below the pit region under the different treatment conditions from three consecutive, independent experiments. Hp, *H pylori*.

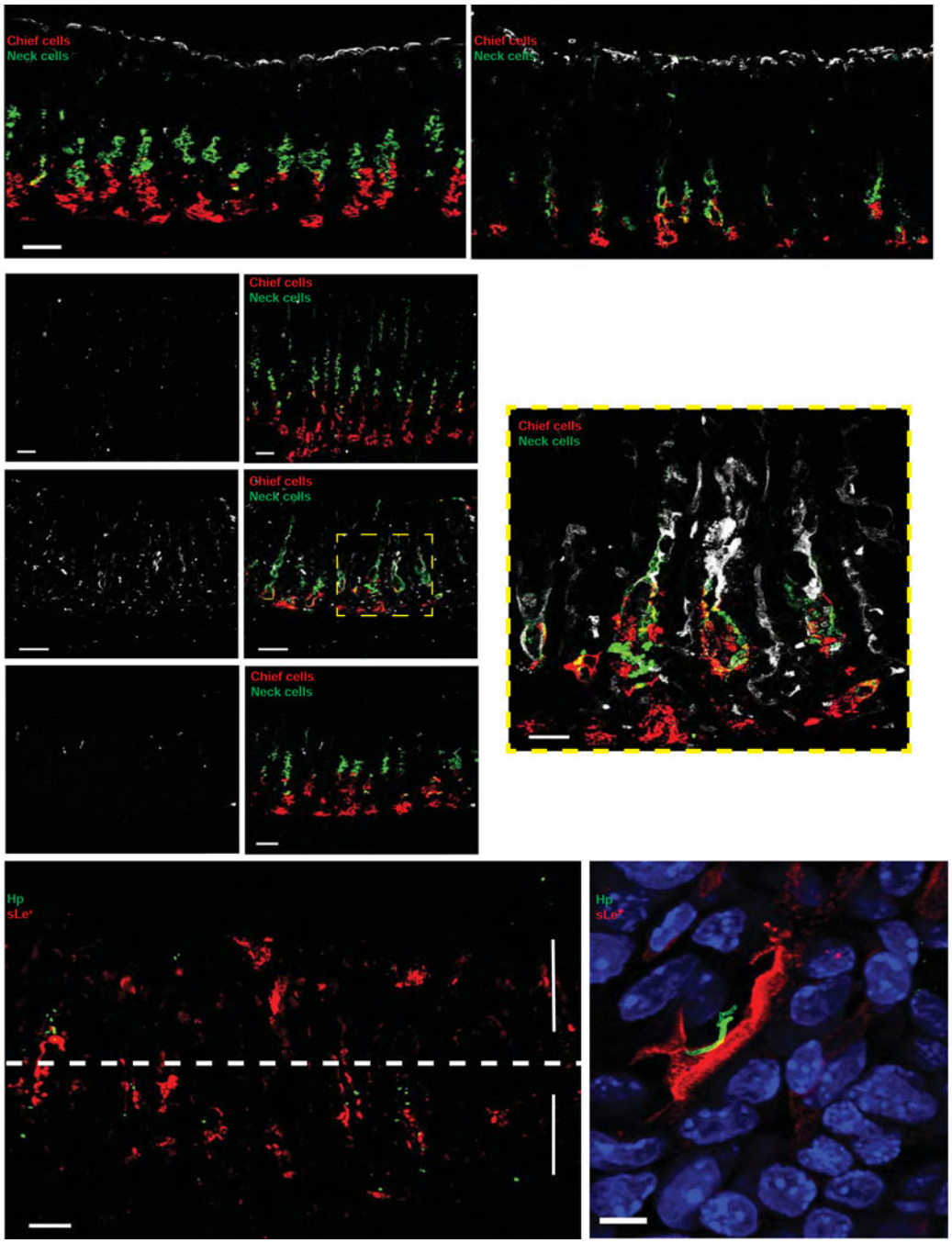

Figure 2. SPEM induces a reversible expansion of sLe^x along the corpus gland axis.

(A) Le^b expression (white) is unchanged following HD-Tam treatment. Representative 100-μm sections of mouse stomachs treated with either vehicle (left) or HD-Tam (right). Scale bars, 50 μm. (B) sLe^x expression (white) extends along the length of SPEM glands (HD-Tam) and co-localizes with metaplastic cells co-expressing chief cell (red) and mucous neck cell (green) markers. This pattern of expression is lost following recovery from HD-Tam injury. Left panels show isolated sLe^x signal from the corresponding, merged right panels. Scale bars, 50 μm (20 μm for boxed image). (C) *H pylori* co-localizes with expanded sLe^x in

SPEM glands *in situ*. *H pylori* (green) penetrate below the pits of SPEM glands, with sLe^x (red) extending along the gland length. The pit and gland regions are highlighted by arrows and separated by a dotted line. Scale bar, 50 μm. (D) Representative image of *H pylori* (green) co-localizing with sLe^x-expressing epithelium (red). Blue, nuclei. Scale bar, 5 μm. Hp, *H pylori*.

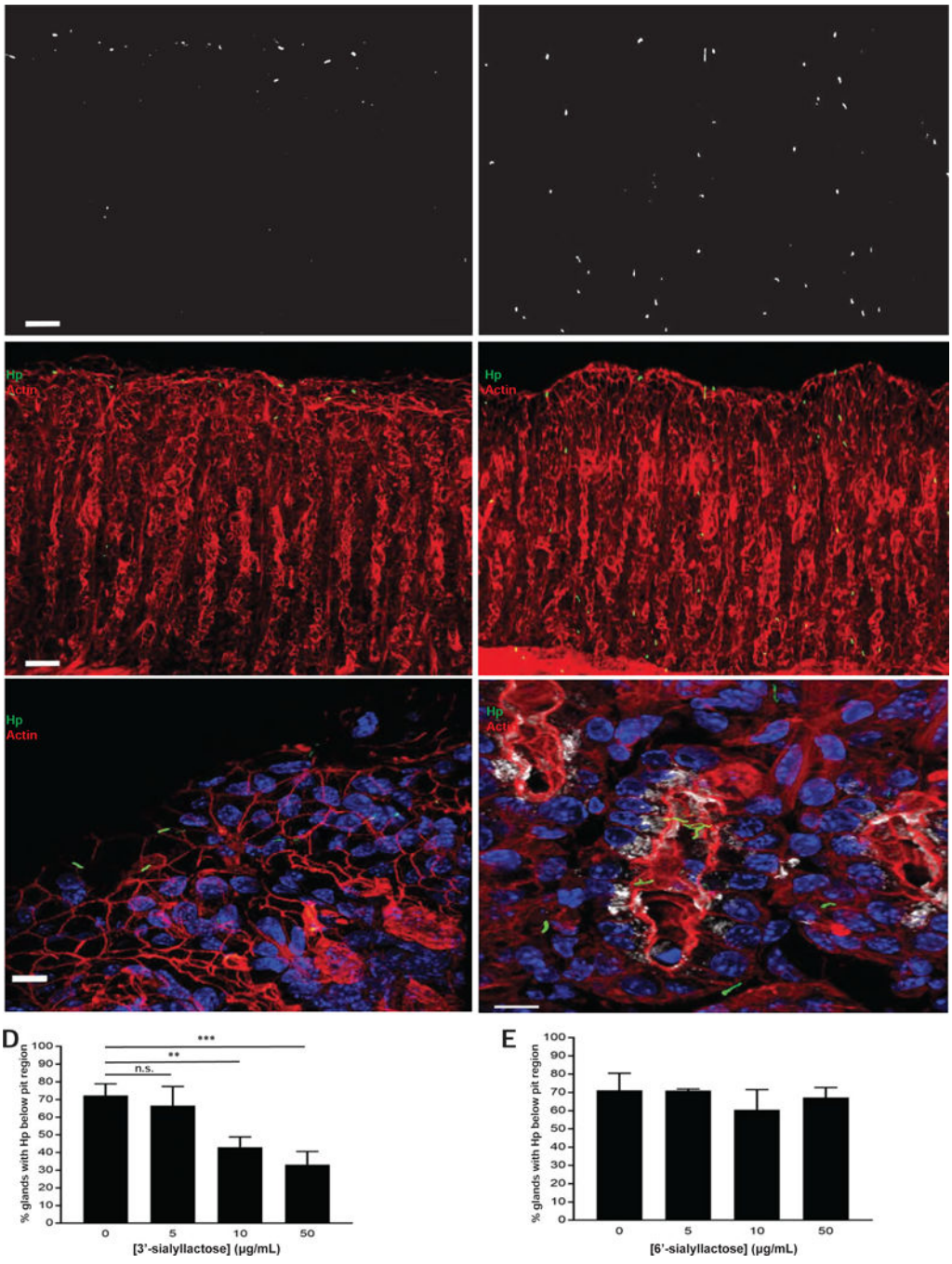

Figure 3. The binding of *H pylori* to SPEM glands *in situ* is α-linkage-specific.

(A–C) 3'-sialyllactose (left), but not 6'-sialyllactose (right), prevents penetration of *H pylori* (green) into SPEM glands. Images in (A) represent isolated *H pylori* signal from the corresponding, merged images in (B). Magnified images in (C) demonstrate that *H pylori* is restricted to the pit in the presence of 3'- sialyllactose but able to access deeper portions of SPEM glands, highlighted by GSII (white), in the presence of 6'-sialyllactose. Blue, nuclei; red, actin. Scale bars, 50 μm for (A) and (B), 5 μm for (C). (D–E) Data show the mean (±SD) percentage of glands containing *H pylori* below the pit region under the different

treatment conditions from three consecutive, independent experiments. For (E), there was no statistically significant difference among any of the tested concentrations relative to the untreated condition. Hp, *H pylori*.

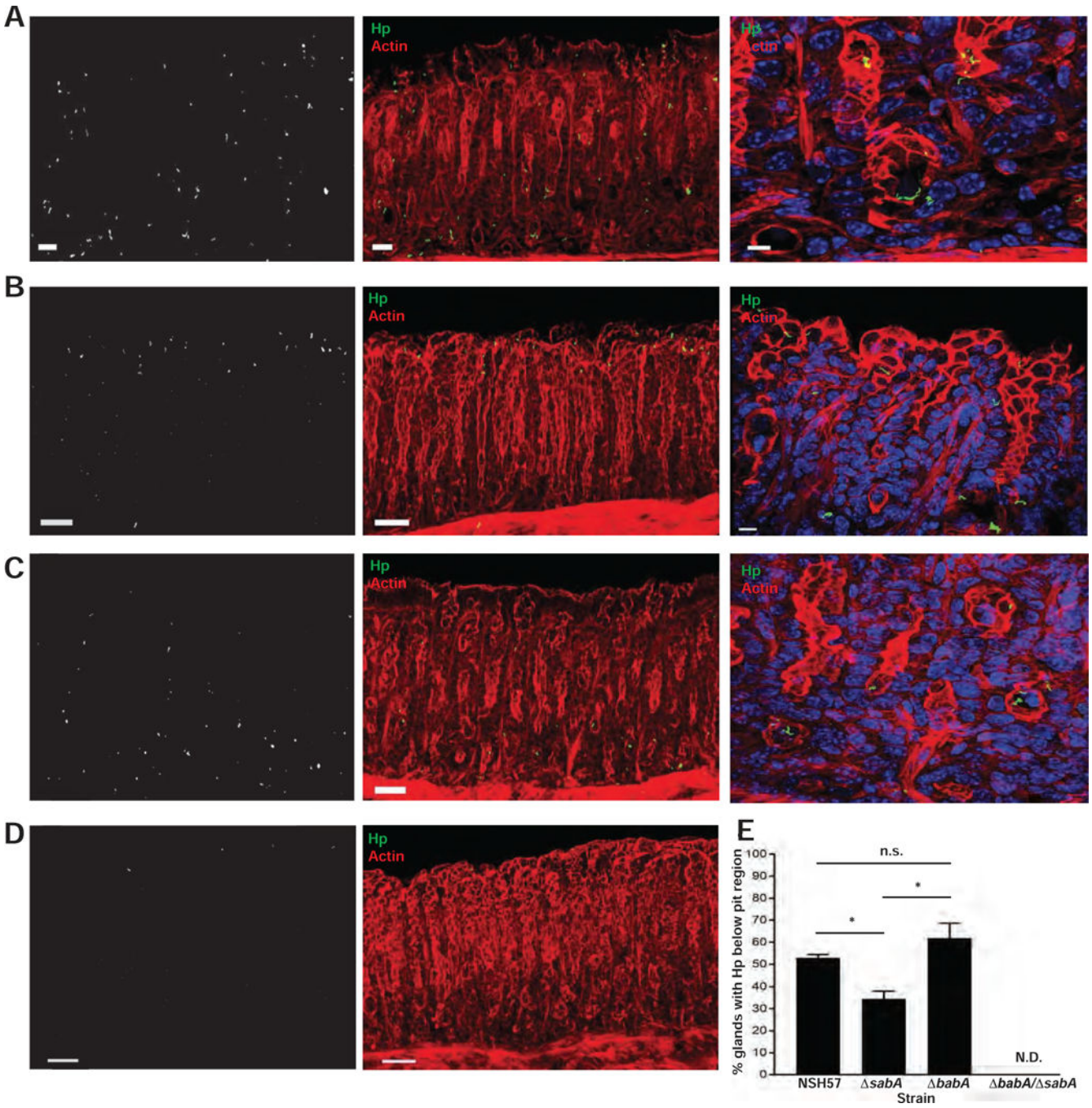

Figure 4. The ability of *H pylori* to bind deep within SPEM glands is largely mediated by SabA.

(A–D) The NSH57 strain (A), or corresponding isogenic mutants (B–D) were incubated with thick gastric corpus sections from mice treated with HD-Tam. The absence of *sabA*, but not *babA*, impairs the ability of *H pylori* to bind deep within SPEM glands. The double mutant lacking both *babA* and *sabA* is unable to effectively bind SPEM glands. Left panels show the isolated *H pylori* signal from the corresponding middle panels. Right panels show magnified images of the corresponding *H pylori* strains (NHS57 and Δ*babA*) binding deep within the gland (labeled base) or confined to the pit (*ΔsabA*). Blue, nuclei; green, *H pylori*;

red, actin. Scale bars, 50 μm (left and middle panels), 5 μm (right panels). (E) Data show the mean (±SD) percentage of glands containing *H pylori* below the pit region for each *H pylori* strain from two consecutive, independent experiments. The *ΔbabA/ΔsabA* double mutant bound fewer than 5% of glands and was not scored (N.D., not determined). Hp, *H pylori*.

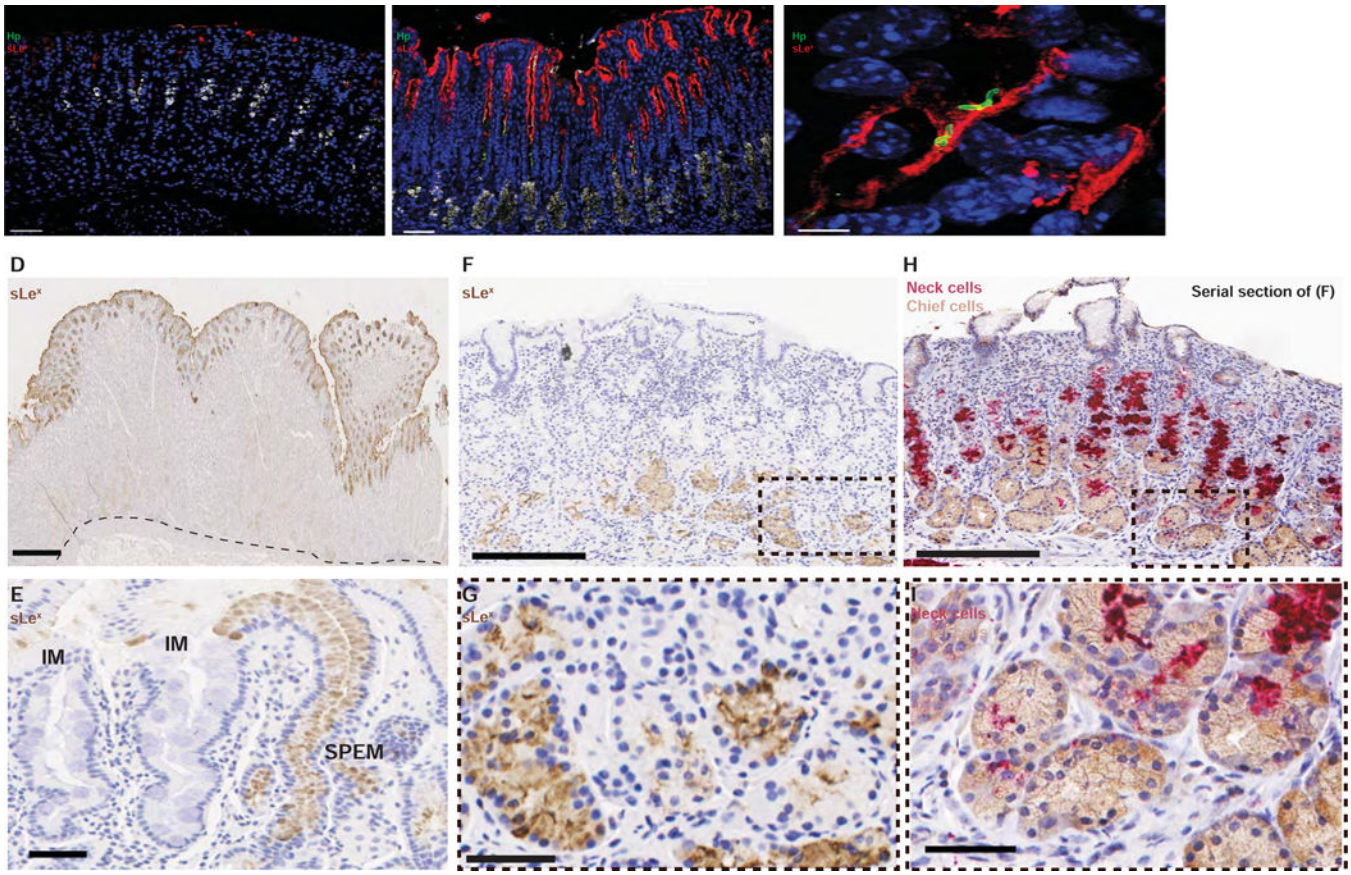

Figure 5. Gastric epithelial expression of sLe^x is expanded in chronic inflammatory conditions in which SPEM occurs.

(A–B) Representative images of a mouse infected with *H pylori* (green) for 6 weeks show enhanced sLe^x expression (red) in colonized glands (B) but scant expression in areas of non-colonized mucosa (A). GSII (white) is in its usual distribution in non-colonized mucosa but at the base in colonized mucosa, indicating SPEM. Scale bars, 50 μm. (C) *H pylori* (green) co-localizes with sLe^x-expressing gastric epithelium (red) *in vivo*. Scale bar, 5 μm. For (A–C), blue marks nuclei. Hp, *H pylori*. (D–I) Histologic sections from human gastric specimens. (D) Normal, *H pylori*-negative gastric tissue from a 36 year-old patient who underwent a bariatric sleeve gastrectomy, stained against sLe^x (brown). The dotted line shows the interface between the gastric epithelium and the muscularis mucosa. Scale bar, 500 μm. (E) Representative image from a gastric biopsy of a 71 year-old *H pylori*-infected patient with chronic atrophic gastritis and focal intestinal metaplasia. sLe^x staining (brown) highlights an area of foveolar hyperplasia in a SPEM gland but is excluded from areas of intestinal metaplasia (IM). Scale bar, 50 μm. (F–I) Representative images from a gastric biopsy of a 67 year-old *H pylori*-infected patient with chronic atrophic gastritis, demonstrating sLe^x staining (F,G) restricted to the bases of SPEM glands, marked by the co-expression of the chief cell (brown) and mucous neck cell (red) markers (panels H and I). (G) and (I) represent magnified images of (F) and (H), respectively. For (F) and (H), scale bars 200 μm; for (G) and (I), scale bars 50 μm.

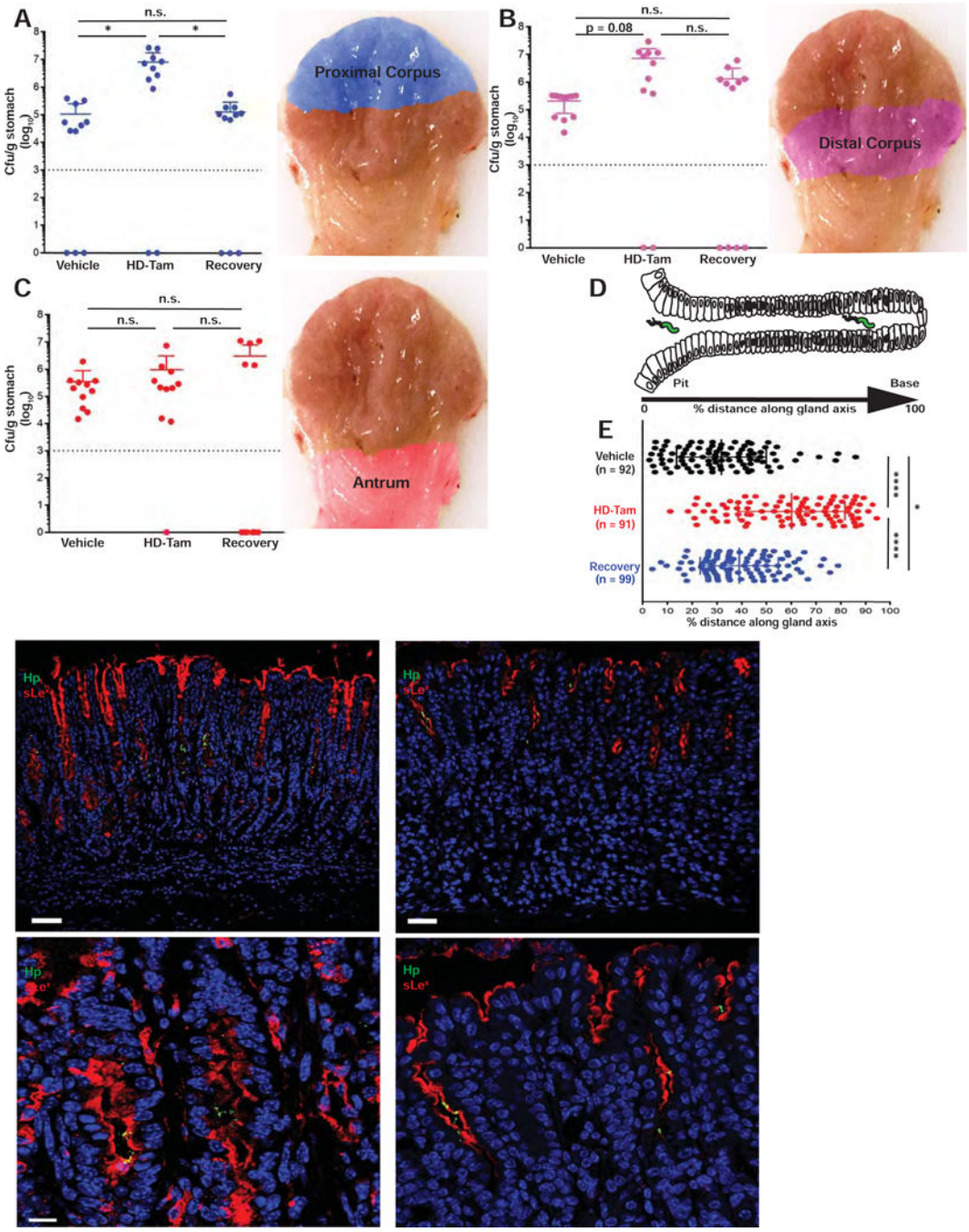

Figure 6. SPEM dictates the topographic and glandular distribution of *H pylori in vivo*.

(A-C) Induction of SPEM allows *H pylori* to more effectively colonize proximal regions of the gastric corpus, and *H pylori* redistributes away from the corpus following recovery from injury. Data represent the mean (±SD) bacterial densities from three pooled, consecutive, independent experiments. Each data point represents a biological replicate. Pseudo-colored anatomic regions used for analysis are shown on right. Dotted line represents the limit of detection. The difference in colonization of the distal corpus between vehicle and HD-Tam treatments shows a trend toward statistical significance (p = 0.08). n.s., not significant (p >

0.1). (D–E) The onset of SPEM alters the glandular distribution of *H pylori in vivo*. The distance of *H pylori* along the gland axis was expressed as a percentage of the total gland length (D). (E) Data represent the mean (±SD) glandular distribution of *H pylori* from three infected littermates/cagemates for each treatment condition. Each data point represents a gland colonized with *H pylori*, with the total numbers of scored glands indicated in parentheses. (F–G) The expansion of sLex (red) and ability of *H pylori* (green) to bind deep within gastric glands are lost following recovery from SPEM. Scale bars, 50 μm. (H–I) Magnified representative images showing *H pylori* co-localizing with sLe^x-expressing gastric epithelium, with *H pylori* binding deeper within SPEM glands following HD-Tam treatment but restricted to the pit following recovery from HD-Tam. Scale bars, 5 μm. For (F–I), blue highlights nuclei. Hp, *H pylori*.

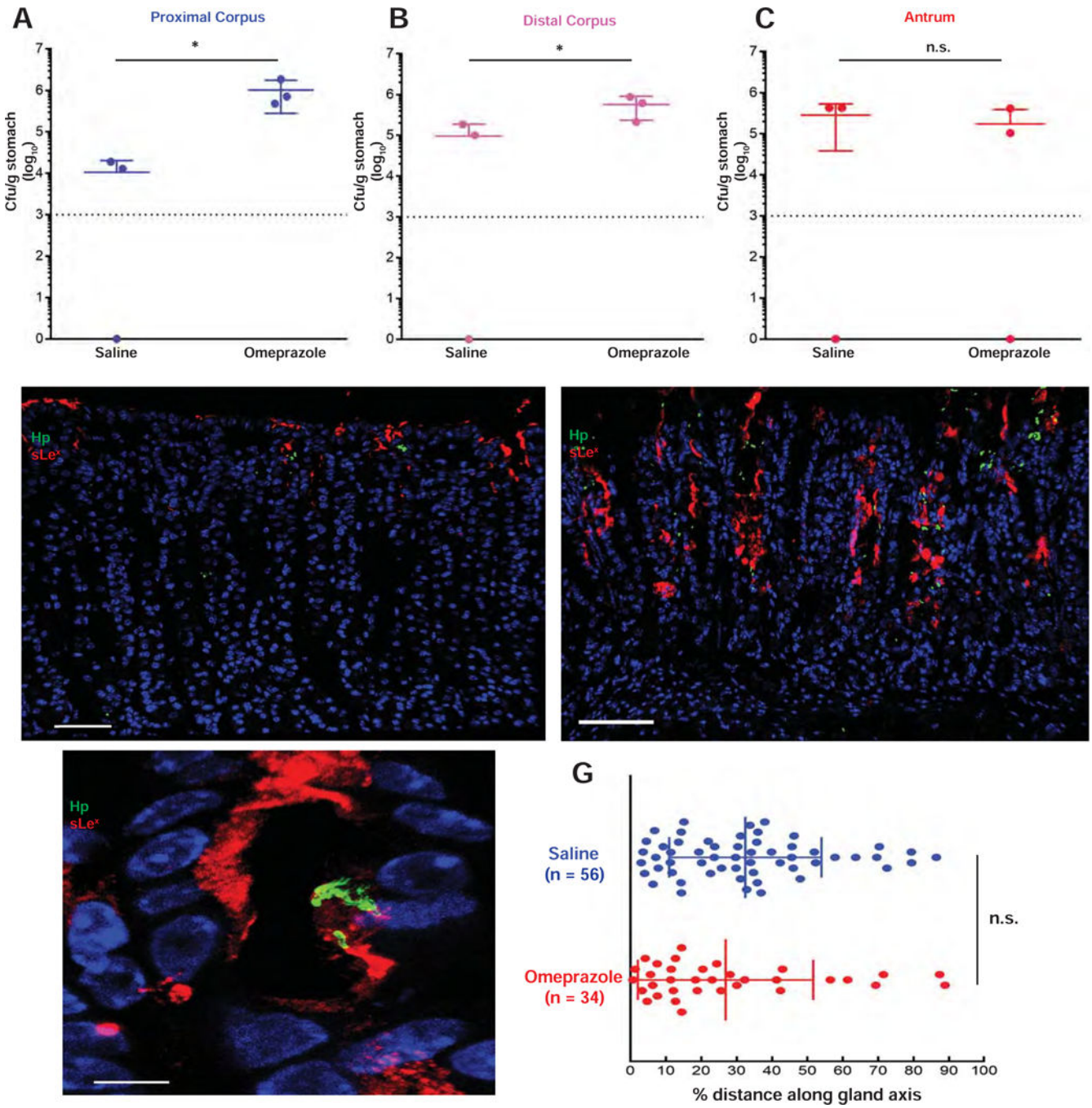

Figure 7. Inhibition of gastric acid alters the topographic, but not the glandular, distribution of *H pylori in vivo*.

(A–C) A representative experiment showing the mean (±SD) bacterial densities from distinct anatomic regions of mice treated with saline or omeprazole. Each data point represents a biological replicate. The dotted line represents the limit of detection. (D–E) Representative images showing that *H pylori* (green) are restricted to the pits in infected, omeprazole-treated mice (D) and that inhibition of gastric acid secretion with omeprazole does not expand sLe^x (red) expression. The onset of SPEM following HD-Tam treatment allows *H pylori* to penetrate deep within SPEM glands demonstrating expanded sLe^x expression (E).

Blue, nuclei. Scale bars, 50 μm. (F) Magnified, representative image shows *H pylori* (green) co-localizing with sLe^x (red) within the pit of an omeprazole-treated mouse. Blue, nuclei. Scale bar, 5 μm. (G) The distance of *H pylori* along the gland axis was expressed as a percentage of total gland length. Data represent the mean (±SD) distribution from three infected littermates/cagemates for each treatment condition. Each data point represents a gland colonized with *H pylori*, with total numbers of scored glands indicated in parentheses. Hp, *H pylori*.